Hardware-in-the-loop testing framework for active accumulator wave energy converters

C. Zeng, J. F. Gaspar, M. J. G. C. Mendes, and C. Guedes Soares

Abstract—**This paper presents a generic hardware-in-the-loop testing framework and taxonomy and their application to a new oil-hydraulic power take-off concept for wave energy converters. In this concept, the charging condition of the oil-hydraulic accumulator is regulated to adapt the damping and stiffness characteristics of the wave energy converter to each sea state condition, to increase the wave energy harvesting performance and conversion efficiency. The present approach is also intended to contribute to the design of hybrid simulations clearly and appropriately since a proper hardware-in-the-loop framework and taxonomy have been not found in the research literature.**

Keywords—**Hardware-in-the-loop simulation, oil-hydraulic technology, power take-off, wave energy converter.**

I. INTRODUCTION

Wave energy converters (WECs) harness and absorb the energy produced by the low-frequency motions of ocean waves and convert it into electrical power to the grid. The conversion is performed by a power take-off (PTO) [1]. Different WEC absorbers and PTO technologies have been proposed. The Oscillating Water Column (OWC) in Fig. 1 [2] captures the wave energy by using the vertical oscillations of the water column to pressurize and depressurize the air inside the absorber and then converting the pneumatic into electrical energy by a biradial air turbine attached to an electric generator and power electronics.

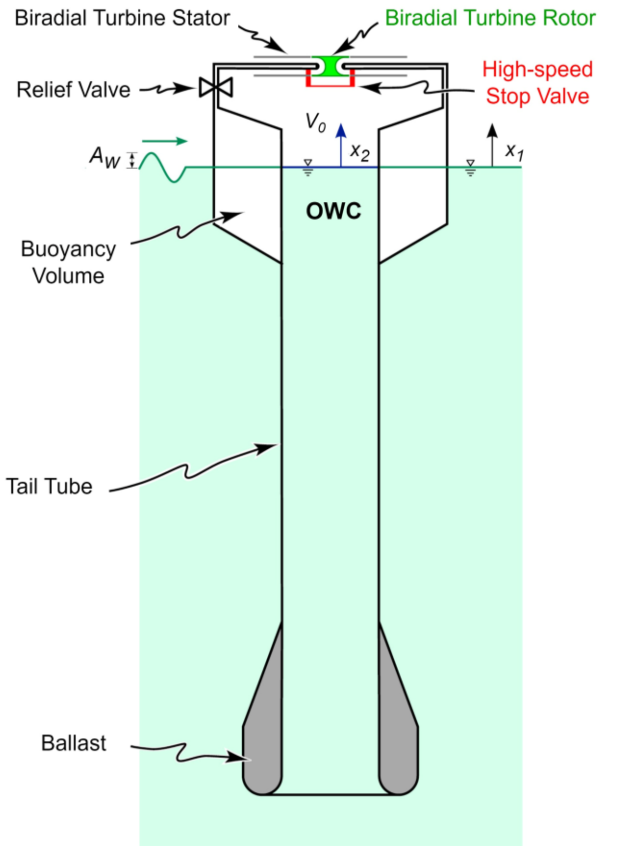

Fig. 1. OWC WEC with a biradial turbine PTO. Legend: (A_W) stands for wave height and (V_0) for initial chamber volume. Adapted from [2].

Another example of a WEC, but using a different absorber and PTO technology is presented in Fig. 2 [3]. The wave energy is captured by the relative mechanical motions of two articulated barges, fore and aft rafts, which are then converted into electrical power by an oil-

This work was performed within the project "Experimental simulation of oil-hydraulic Power Take-Off systems for Wave Energy Converters", funded by Portuguese Foundation for Science and Technology (FCT) under contract PTDC/EME-REN/29044/2017 and project "Variable geometry Wave Energy Conversion system for floating platforms" funded by FCT under contract PTDC/EME-REN/0242/2020. The work contributes to the Strategic Research Plan of the Centre for Marine Technology and Ocean Engineering, which is financed by the Portuguese Foundation for Science and Technology (Fundação para a Ciência e Tecnologia-FCT) under contract UIDB/UIDP/00134/2020.

C. Zeng, J. F. Gaspar, M. J. G. C. Mendes and C. Guedes Soares are with the Centre for Marine Technology and Ocean Engineering (CENTEC), Instituto Superior Técnico, Universidade de Lisboa, Avenida Rovisco Pais, 1049-001 Lisboa, Portugal, e-mails: chen.zeng; jose.gaspar; mario.mendes; c.guedes.soares@centec.tecnico.ulisboa.pt

M. J. G. C. Mendes is also with CIMOSM - Instituto Superior de Engenharia de Lisboa (ISEL), Instituto Politécnico de Lisboa, Rua Conselheiro Emídio Navarro 1, 1959-007 Lisboa, Portugal (email: mario.mendes@isel.pt)

Digital Object Identifier: https://doi.org/10.36688/ewtec-2023-430

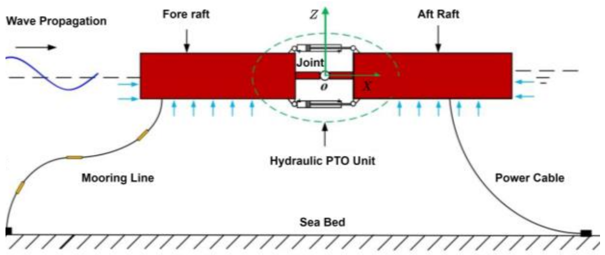

Fig. 2. Two-raft oil-hydraulic PTO. Adapted from [3].

hydraulic PTO, consisting of two hydraulic cylinders attached to a hydrostatic transmission, electrical generator and power electronics.

The development of these devices presents big challenges, because of the expensive and risky testing of real devices in real conditions (wave tanks and open sea) and the difficulty in numerically modelling some physical phenomena and components and simulating them exactly in an adequate time frame [4]–[6]. Thus, hardware-in-the-loop (HIL) simulation has been proposed to take advantage of the benefits of using hybrid models where real physical and numerical (virtual) parts of the device are used, in other words, physical components that are hard to numerically model, together with numerical models of components that are expensive to build or test [7]. For example, real components of the WEC prototype may be the PTO and its controller whereas the virtual ones are the WEC absorber and the sea wave resource.

As a result, HIL has been increasingly adopted in this field of research [1], [8]–[10], because it is considered a cost-effective approach for the development of WEC, PTO and PTO controllers, analysis and validation of PTO dynamics, performance and efficiency, and the calibration of mathematical models. Moreover, it allows a safer, more controlled, replicable testing environment, with a thorough reduction in operational risks, price, and execution time frame [4]–[6].

These HIL methodologies are represented with diagrams like the one presented in Fig. 3, which shows the HIL approach for the dry testing of the OWC WEC (Figs 1 and 4). The real physical parts are the electrical generator, power converter, PLC, IDMEC/IST control law and connections to the electrical grid whereas the virtual ones are the wave resource, WEC absorber and biradial turbine numerical models that run in real-time and inside the xPC target computer.

The real parts are included inside a domain named the “Tecnalia Test Rig (Model Scale)” whereas the virtual ones are inside the “Hardware-in-the-loop simulation and data logging (prototype scale)” domain (Fig. 3). The interaction between these domains is performed by sending to the motor power converter a signal that corresponds to the torque generated by the air turbine on the electrical generator and receiving back a rotational speed signal to update the turbine numerical model. Thus, the turbine action on the generator is simulated but the turbine itself

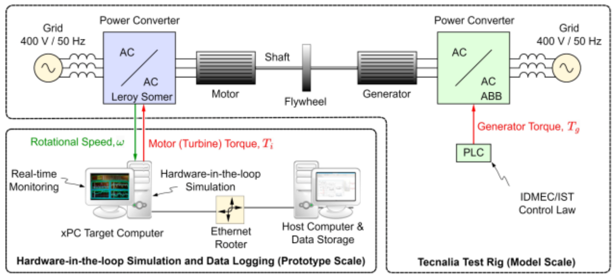

Fig. 3. OWC HIL representation. Legend: (PLC) stands for Programmable Logic Computer and (AC) for Alternating Current. Adapted from [2].

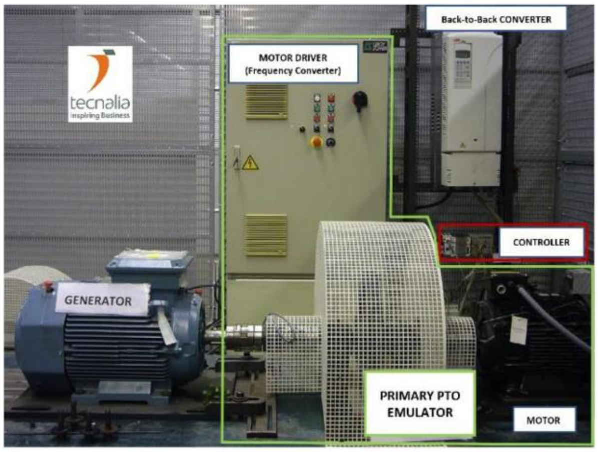

Fig. 4. Tecnalia Electrical PTO test rig. Adapted from [5].

is not physically present in the test rig. Thus, the electrical motor and associated parts cannot be confused with the OWC real parts domain. However, the representation does not give this indication, by including these parts as belonging to the “model scale” domain.

Another methodological representation of the same HIL test rig can be found in the diagram presented in Fig. 5. Here, the representation domains are named differently, "Emulated components” and “real embedded components” for virtual and real physical parts.

Thus, the electrical motor and associated parts are separated from the real tested parts of the WEC, however, are included in the same domain as the virtual parts (Fig. 5) [15]. Hence, these parts are not real in the sense of the parts that are under test, but the diagram does not indicate that they are not virtual as well. These two diagrams are a good example of the need to clarify the boundary between real physical and virtual parts of the WEC prototype.

The diagram presented in Fig. 6 describes the HIL methodology for the dry testing of the two-raft WEC (Figs 2 and 7). It shows an intention to clarify the separation between real (“Real Plan” domain) and virtual (“Simulated Parts” domain) parts of the WEC, which is better than the previous cases (Figs. 3 and 5) but is still not complete. The “Hydraulic Power Pack System” subdomain implements the physical actions of the

"Software Model and Controller" subdomain (virtual part) on the "Hydraulic PTO unit" (real part domain) but is indicated as belonging to the same domain where the virtual part of the WEC is included. It should stand isolated as a third domain that performs the interfacing between the real and virtual part domains.

A preliminary review in the research literature dedicated to HIL methodologies applied on WECs, and conducted by [11], confirms the existence of ill-defined boundaries between WEC virtual and real part domains and diverse terms for the same methodological objects. Hence, the study proposes a methodological representation framework and consensual terminology for the development of systematic and clear descriptions of the HIL applications [11]. The framework consists of three domains: the Simulated, Real and Simulated – Real parts interface domains. The simulated parts domain is about the numerical models of the WEC subsystems or parts, like PTO hardware and control algorithms, that are converted by dedicated software to a real-time model, which is then loaded on a real-time simulation machine.

The real parts domain includes embedded WEC subsystems or parts, like hardware, controller and control algorithms, that are real physical parts under experimental testing. Thus, these parts are also named devices under test or target hardware, controller and target control algorithms. The target control algorithms are developed, compiled and loaded to the target controller by development software running in a development computer.

The Simulated – Real parts interface domain includes the system hardware and software that physically implement the actions of the numerically simulated parts on the embedded ones. This system is named the emulator interface and is made of a controller, control algorithm, power electronics and electrical driver.

A compensator may be added to the emulator system to adjust the dynamic differences added by the emulator in the testing. For example, the interface emulator made of a power inverter, electrical motor and flywheel, as shown in Figs 3 and 5, may have a different dynamic characteristic of the biradial turbine, thus, not providing a reliable torque on the target generator. Moreover, a compensator may be added on the emulator interface represented as the "Hydraulic Power Pack System" in Fig. 6, if it has dynamic characteristics that affect the actuation of the target PTO with a force that must faithfully represent the excitation force produced by the fore and aft rafts. So, this shows, why it is so important to represent the emulator system separated from the Simulated and Real part domains.

The same study also reveals that HIL methodologies may be represented with different levels of information, some more abstract and logical than others, more technologically oriented [11]. Thus, the actionability term is introduced to indicate the kind of information contained in these HIL representations.

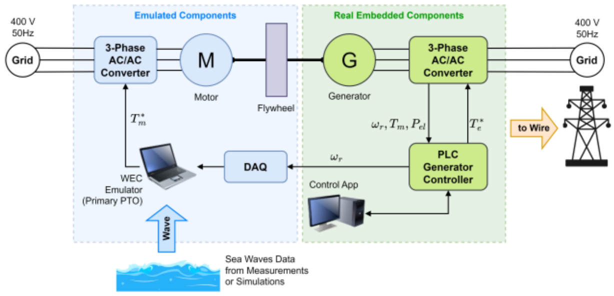

Fig. 5. OWC HIL representation. Legend: (T_m) stands for mechanical torque, (ω_r) for rotational speed, (P_{el}) for electrical power, and (T_e) for electrical torque. Adapted from [5].

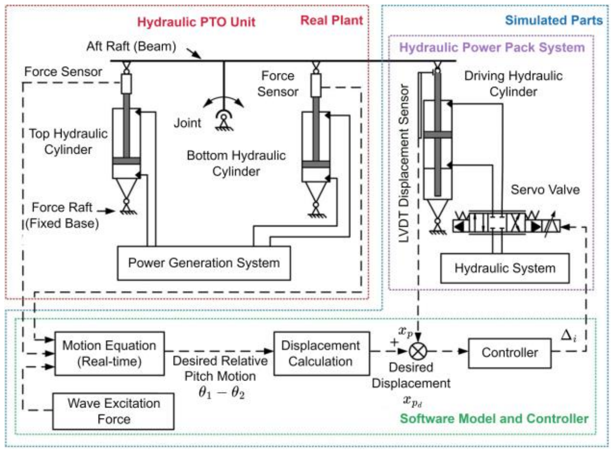

Fig. 6. Two-raft WEC HIL representation. Legend: (x_p) stands for cylinder rod displacement, (x_{p_d}) for desired displacement, (θ_1) for pitch displacement of the fore raft, (θ_2) for pitch displacement of the aft raft, (Δ_i) for current delta and (LVDT) for the Linear Variable Differential Transformer. Adapted from [3].

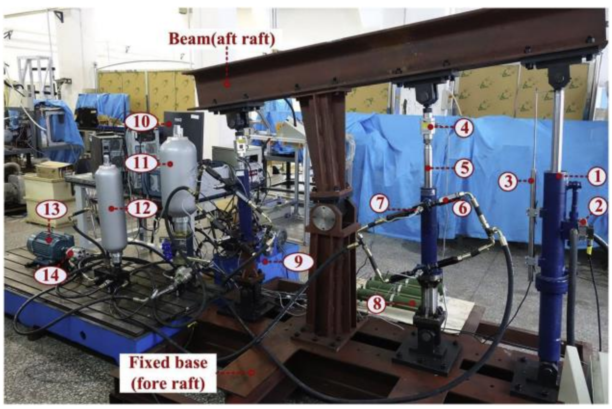

Fig. 7. Two-raft oil-hydraulic PTO test rig. Adapted from [3].

Actionability term stands for the "ability of information to indicate specific actions to be taken to achieve the desired objective" [12], [13]. Thus, the more actionable the information is, the easier the implementation of the HIL approach at the technological level, and the more abstract the information is, the less actionable is for technical concretization. Therefore, the utilization of different actionality representations of the same HIL methodology depends on the objective at hand, such as having a wider and immediate understanding of the methodology, with a more abstract representation, or a narrower one to understand how is technologically implemented by using a less abstract but more actionable and technological representation. Moreover, the utilization of both representations provides an additional and holistic understating of the HIL setup as well.

This paper aims to present results from a literature review intended to continue the development of the HIL methodological framework and taxonomy and articulate it with a case study. The paper is organized into six sections. In Section II, the HIL methodological framework and taxonomy are presented, then the case study is presented in Section III and the HIL approach for the testing of the PTO concept is presented in Section IV. Then, the paper results are discussed and summarized. in the conclusions.

II. HIL METHODOLOGICAL FRAMEWORK

This section is organized into two subsections, the first dedicated to the methodological framework and the second to more detailed and technical issues that must be considered for the HIL application.

A. *Methodological framework*

The analysis of the terminologies used in the description of HIL methodologies resulted in the collection of ninety terms that are added to the three terms described in the introduction section (simulated, real and simulated – real parts interface domains). The terms are listed and described in Table 1.

These terms are hierarchically related. The "host computer" term contains "real-time simulation machine" and "simulation software" terms. The first includes "real-time simulation" and "simulated parts domain" terms. The latter include "real-time code" and "simulated part" terms. The "simulation software" term contains the "simulation model", "compiler" and "real-time model" terminology. The "real parts domain" clusters the "device under test", "embedded part", "target hardware", "target controller" and "target algorithm" terms and the "interface part domain" the "emulator interface", "interface control algorithm" and "interface compensator" terms.

The technology that has been used to implement the HIL approach was also reviewed and the most relevant devices and software have been collected and organized according to the presented terminology, as presented in Table II. It was found that a real-time simulation machine may be integrated into a host computer as an input/output (I/O) board (e.g. dSPACE DS1104) or operate as a standalone unit. Moreover, the real time simulation machine may be used as one part of the emulator interface, because has inside controllers that run control algorithms and communicate with actuators and sensors.

TABLE I
HIL TERMINOLOGY

Term	Description
Compiler	Software that converts the numerical model into an RT model.
Development Computer	Contains the development software and interacts with the target controller
Development Software	Software to develop, compile and load the control algorithm into the target controller
DuT	Embedded device under experimental testing
Embedded part	Real physical subsystem/part
Emulator Interface	Emulates the physical action of the RT model on the target hardware or target controller.
Host computer	Contains the sim. software, RT model and RTSM
Interface control algorithm	Algorithm developed and compiled in the host computer and loaded in the emulator controller
Interface compensator	Ensures an accurate emulation of the physical actions of the RT model on the target hardware
Interface domain	The domain that contains the system that simulates the physical actions of the numerically simulated parts on the embedded ones
Real parts domain	The domain that contains the embedded WEC subsystems or parts
RT code	RT model code that is loaded into the RTSM
RT model	The real-time version of the simulation model
RTS	Real-time simulation
RTSM	RTS high-speed processing machine
Sim. model	Numerical model of the simulated subsystem/part
Simulated part	Numerically simulated subsystem/part
Simulated parts domain	The domain that contains the numerical models of the WEC subsystems or parts
Sim. software	Tool for model development and compilation
Target hardware	The hardware under experimental testing
Target controller	The controller under experimental testing
Target algorithm	The control algorithm under experimental testing

Thus, researchers may use the terminology (Table I) to build high-level logical, or abstract representations of the HIL methodology for a specific application and then produce complementary and more actionable representations to execute the designed methodology, by using Table II. Thus, it is recommendable to build logical and technical representations of the HIL application to

TABLE II
HIL TECHNOLOGY

Term	Technologies
Compiler	dSPACE Control Desk, Matlab xPC target RT, RT Labview and Simulink RT [6], [14]–[16]
Development Computer	Personal computer
Development Software	Beckhoff simulation target, LabView RT target, Matlab xPC RT target and Simulink RT [17], [18]
Emulator Interface	Cylinder-piston drive and DC motor [16], [19]
Host computer	Personal computer, Beckhoff PLC [20]
Interface compensator	Friction-model-based feed-forward compensator and PI (proportional–integrative) [21]
RTSM	dSPACE DS1006, DS1103, DS1104 [19], [22], [23]
Sim. software	Matlab and Simulink, SimMechanics, Simscape and NI Veristand [7], [14]–[16]
Target hardware	DC generator and AC/AC converter [2], [14]
Target controller	Beckhoff CXI020, NI6221, S7-300 [14], [17], [23]–[25]

have a more comprehensive view and understating of the testing approach.

B. *Issue and solution to phase delay*

It is important to carefully evaluate the requirements of WECs and HIL simulation setup when choosing RT hardware. Factors such as computational power, I/O capabilities, RT performance, cost and compatibility with simulation tools should be taken into consideration. Furthermore, when RT hardware is needed, it is crucial to assess the hardware's ability to handle the phase delay or time step introduced by the RTS and sensors. The RT hardware should have sufficient processing power to handle the computational load of the simulation model within the desired time step. Higher processing power enables smaller time steps, reducing the phase delay. The hardware's I/O latency should be minimized to ensure accurate and timely communication between the simulation and external devices, such as sensors and actuators. Lower I/O latency reduces the overall phase delay in the system. The hardware should support high sampling rates for acquiring sensor data and actuator control signals. A higher sampling rate allows for more frequent updates and reduces the phase delay caused by sensor measurements. The RT hardware should employ a reliable and deterministic RT operating system to ensure precise timing and minimize delays. Also, the hardware should be eased to integrate with the simulation software tools and it should be available with appropriate drivers or interfaces. Compatibility with widely used simulation environments, such as Simulink or LabVIEW, can simplify the development and deployment process. Finally, it is important to have some scalability and expandability in the HIL setup, depending on the complexity and future expansion plans for the HIL setup, it is important to assess whether the chosen hardware can accommodate additional components, interfaces, or modules if required. Concluding, the choice of RT hardware should be aligned with the specific needs and constraints of the wave energy HIL simulation.

The RTS plays a crucial role in a HIL experiment and the phase delay introduced in the RTS is essential for achieving accurate and reliable results. The following contents of this section will introduce some possible methods that can mitigate the phase delay introduced in the RTS, focusing on numerical methods and hardware selection.

1) *Numerical method for phase delay mitigation*

In HIL simulations, the phase delay is often amplified by the increasing complexity of the numerical model used. To address this challenge, it is important to balance between accuracy and computational efficiency when selecting the numerical model and consider appropriate simplifications where possible.

The dynamics of the WEC prime mover in waves are numerically modelled in the HIL experiment for WEC PTOs. The equations of motion are employed to describe the kinematics of the prime mover. The hydrodynamic simulations commonly require much higher computational effort. Therefore, the hydrodynamic performance of the prime mover can be simulated by the frequency domain linear boundary element solver, such as WAMIT and NEMOH, in advance. Then the state-space impulse functions can be derived from the hydrodynamic performance for the following time-domain simulations, leading to a reduced computational requirement [26], [27].

In addition, there is a method known as delay compensation which accounts for delay time in the actuator control and estimates its future behaviour for delay compensation, to improve the accuracy of the HIL simulation and control [28].

2) *Real-time hardware selection*

The RT simulator is a crucial component in the HIL setup. It emulates the behaviour of the physical system or environment where the control system will ultimately be deployed. The simulator typically runs on a powerful computer and executes the mathematical models representing the virtual parts in real-time. It generates sensor signals and responds to control commands from the control system. Several RT simulators are widely used, including dSPACE DS1104, National Instrument (NI) RT hardware, Speedgoat and suitable Field-Programmable Gate Arrays (FPGAs). In addition, Raspberry Pi is gaining popularity as a low-end RT simulator. Each of these simulators offers unique features and capabilities for RTS and HIL testing which are discussed in the following content:

1) dSPACE DS1104: the simulator is well-established and widely used in the industry and research. It offers a comprehensive set of hardware and software tools for RTS and HIL experiments and provides high-performance RT execution and supports complex simulation models. But it is relatively expensive. [29], [30]
2) NI RT hardware, such as CompactRIO,: with its RT processor and FPGA, CompactRIO can execute RTS tasks. The RT processor runs a deterministic operating system and allows for the execution of control algorithms and mathematical models with low latency and deterministic timing. The FPGA provides hardware-level parallelism and can be programmed to accelerate computations or handle specific RT tasks. To perform RTS on a CompactRIO system, it would typically develop or import mathematical models into software such as LabVIEW or LabVIEW RT Module. But it has limited flexibility in terms of customization and integration with third-party tools or hardware. It is more commonly used for HIL testing, where it operates as the hardware interface between the real physical system and the simulation models or control algorithms. Compared to dedicated RT simulators, the RT simulation capabilities of CompactRIO may have certain limitations. [31]
3) Speedgoat target machine: this platform provides RT target machines specifically designed for HIL simulations. These systems are based on powerful multi-core processors and offer high-speed I/O interfaces. Speedgoat target machine seamlessly integrates with Matlab and Simulink. However, it offers limited support for non-MATLAB/Simulink-based models or simulations. In addition, it requires the purchase of additional hardware targets or custom RT systems. [32]
4) Raspberry Pi-based Systems: This board and system is a popular and affordable single-board computer that can be utilized for RTS. It offers a cost-effective solution for small-scale HIL setups. However, the processing power and I/O capabilities of Raspberry Pi might be limited compared to high-end alternatives. RT performance might be affected in complex simulations or large-scale systems. [33]
5) FPGAs: FPGAs are hardware devices that can be programmed to perform specific RT tasks. These devices offer high-speed and low-latency processing, making them suitable for RTS. FPGAs can be used in combination with other hardware platforms to accelerate computationally intensive tasks. However, programming and implementing FPGA-based solutions can be complex and require specialized expertise. [34, 35]

The advantages and disadvantages mentioned above are, of course, general characteristics and may vary depending on specific hardware models, versions, and configurations within each platform. Depending on project requirements, budget, and available expertise is essential when selecting the most suitable hardware platform for the WEC HIL simulation.

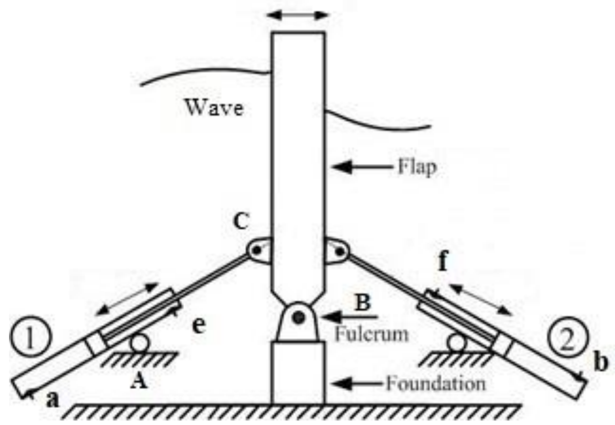

Fig. 8. Surge WEC absorber attached to an oil hydrostatic transmission (Grant contract PTDC/EME-REN/29044/2017). Legend: (1, 2) asymmetric cylinders, (A) cylinder trunnion joint, (B) WEC fulcrum joint, (C) cylinder clevis joint, (a, b) cylinder rodless chamber ports, and (e, f) are the cylinder rod chamber ports.

III. CASE STUDY

The PTO concept is presented adapted to a Surge WEC absorber in Figs 8 and 9 [36]. The interface between the absorber and the PTO is performed with two asymmetric oil-hydraulic cylinders (#1 and #2) that operate as one symmetric cylinder, since a direct connection is performed between rod chamber ports (e and f) and only the rodless chambers are connected to the PTO (a and b ports).

As presented in Fig. 9, the hydraulic power received from hydraulic cylinders (Fig. 8) is rectified by high-pressure check valves (HCV) and is delivered to the PTO high-pressure side. The low-pressure check valves (LCV) supply the low-pressure side of the hydraulic cylinders with an oil flow rate identical to the one on the high-pressure side. The low-pressure level is assured by a pressure-controlled pump (P1) assisted by a low-pressure accumulator (LPA).

The hydraulic power is converted into mechanical power in the shaft shared by two hydraulic motors, named first (HM1) and second-stage (HM2) motors. HM1 is operated to perform continuous control of the hydraulic cylinder forces at low energy wave groups of a specific sea state condition, thus in a specific range of variable oil pressures. These oil pressures are below the one and relatively more stable oil pressure on the second-stage side, keeping the high-pressure bypass check valve (HCV2) closed and the first and second-stage hydraulic transmissions, decoupled. The hydraulic motor HM2 discharges oil from the main high-pressure accumulator

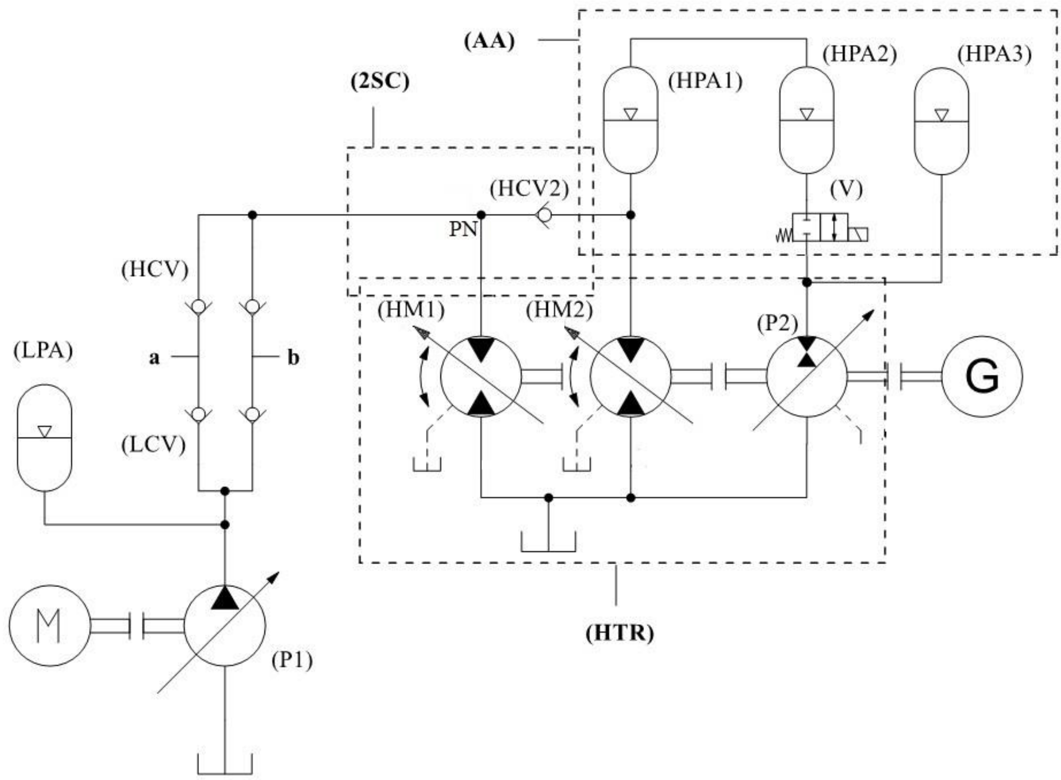

Fig. 9. Hybrid and active accumulator PTO (Grant contract PTDC/EME-REN/29044/2017). Legend: (HCV) high-pressure check valve, (HCV2) high-pressure bypass check valve, (HM1) first stage hydraulic motor HM, (HM2) second stage hydraulic motor, (HPA1) main high-pressure accumulator, (HPA2) high-pressure auxiliary accumulator, (HPA3) backup HPA, (HTR) oil-hydraulic transformer, (LCV) low-pressure check valve, (M) electrical motor, (PN) Pressure Node, (P1) boost pump, (P2) charging pump and (V) is a cut-off valve.

(HPA1) and converts this hydraulic power into mechanical power on the drive shaft (HM1).

The control of the HM1 operation is passed over to the HM2 when HCV2 is open, which means that oil pressures are above the second-stage pressure. This happens when the oil flows produced by hydraulic cylinders overcome the capacity of the HM1, thus leading to the saturation of this unit and compression of the oil that must escape somewhere (safety valves are provided in case of HCV2 malfunction, but are not shown in Fig 9). Consequently, the HPA1 is charged whereas the remaining oil flow is diverted to HM2. The control of the cylinder forces is then limited because adjustments in HM2 are undermined by HPA1. These conditions are caused by higher energy wave groups of a specific sea state condition.

The control limitations in the second-stage side may be minimized by varying the HPA1 stiffness, which is achieved by adjusting the oil volume inside the high-pressure auxiliary accumulator (HPA2), in other words, changing the compressibility level of the gas shared by HPA1 and HPA2 gas chambers. Additional damping effects may be provided when the HPA2 displaced oil flow is converted into mechanical power to the shaft by the charging pump (P2), operating in this case as a motor.

P2 is assisted by the backup accumulator (HPA3) when the discharged oil overcomes the P2 capacity. The cut-off valve is open whenever these adjustments are required.

The adaption of the PTO to different sea state conditions is performed by adjusting the maximum HM1 displacement (within 70 to 100%), in other words, the maximum oil flow capacity and the pressure level on the second-stage side. Thus, this sets the conditions for the opening of HCV2 for different sea state conditions.

The control of the HM1, when decoupled from the second-stage side, is performed to avoid oil compressibility effects added by the big-size oil-hydraulic accumulator (HPA1) in the control system. These effects are noticeable at lower than higher oil pressures. Thus, the two stages are hydraulically coupled when the oil pressure in the first stage goes up until a certain level, where the compressibility effects are less harmful to the control system.

The objective of the two-stage approach is also to minimize the negative impact on the hydraulic to mechanical-power conversion efficiency by allowing HM1 to operate in a wider displacement span (0 to 100%) than HM2 (70 to 100%). This is because the impact on the PTO global conversion efficiency is less noticeable when using a comparatively smaller size HM1 operating with low energetic waves group, whereas the biggest part of the conversion energy is provided by HM2 (at the most energetic group of waves). Moreover, the HM1 is already operating at its maximum efficiency when the two stages are hydraulically coupled since the HM1 maximum

Fig. 10. Oil-hydraulic HIL test rig for testing the hybrid and active accumulator PTO concept (Grant contract PTDC/EME-REN/29044/2017).

Fig. 11. Oil-hydraulic HIL test rig. Back view (Grant contract PTDC/EME-REN/29044/2017).

displacement is set between 70 to 100 %, depending on the sea state condition.

The HIL test rig is presented in Figs 10 and 11. The target hardware is located on the top side and behind the oil tank (red painted box). This hardware includes the HPA1, HPA2 (two small blue-coloured accumulators), and the HM2 (attached to the front curved, red-coloured vertical plate). The HM2 unit may operate as HM1, by a valve that cuts off the connection between HM2 and HPA1. The target PTO controller is an industrial PLC installed inside a grey switchboard (located on the left side of the oil tank). The PLC may be locally or remotely connected to a development computer, which contains the PLC proprietary development software. The HM1, HM2, P1, P2, V and G target control algorithms run inside the PLC.

The simulated parts run inside an RTSM, also installed inside the switchboard. These parts are the WEC absorber and mechanical interface with the PTO hydraulic cylinders (Fig. 8), the oil boost system (M, P1 and LPA in Fig. 9), the rectification system (LCV and HCV), bypass valve HCV2, HPA2 charging system (P2, V and HPA3) and generator (G). The HM1 is also a simulated part when HM2 is operated as the target hardware and vice-versa.

Three emulator interfaces are installed in the test rig. The first one physically implements the actions of the simulated parts on the HM2. It receives a signal from the RSTM that corresponds to the HCV2 simulated oil flow (that comes from the hydraulic cylinders). The emulator consists of a controller that compares this signal with the one sent by an oil flow sensor located at the outlet of a proportional valve. This valve modulates the oil flow supplied by the hydraulic power unit and supplies it to the HM2, according to the signal received from the controller. The power unit is located between the switchboard and HM2. It has the biggest and highest accumulator in the rig, because of its capacity to supply big oil flow peaks to the emulator.

The second emulator interface implements the physical actions of the simulated generator (G), charging pump (P2) and HTR shaft on HM2. The HM2 may be also considered as one of the simulated parts in case of testing HM1 as the target hardware. Thus, the emulator receives a signal from the RSTM that corresponds to the summation of the G, P1 and HM1 (or HM2) torques. The emulator consists of a controller that compares the torque signal with one determined from calculations performed on signals received from an oil pump connected to the HM2 shaft (not visible in Fig. 9). The pump operates as a hydraulic breaker to provide the resistant torque that corresponds to the signal received from the controller.

The third emulator interface implements the physical actions of the simulated charging system (V, P2 and HPA 3) on the active oil-hydraulic accumulator. The emulator receives a signal from the RSTM that corresponds to the HPA2 simulated oil flow (that comes from the P2 and HPA). A controller compares this signal with the one sent by a flow sensor located at the outlet of the proportional valve. This valve modulates the oil flow that comes from the rig power unit and supplies it to the HPA2, according to the signal received from the controller. Note that this is not the same hydraulic circuit of the first presented emulator, despite sharing the same power unit.

The RTSM is used to run the emulator controllers and compensators and communicates with the target PLC to test the P1, P2, V and G target control algorithms since these units are simulated in the RTSM (by an RT model). Moreover, it communicates with the PLC to test the HM1 or HM2 target control algorithms when HM1 or HM2 is a simulated part, respectively. This means that one target control algorithm is in direct contact with the target hydraulic motor HM2 whereas the other control algorithm with a simulated version of unit HM1, and vice-versa.

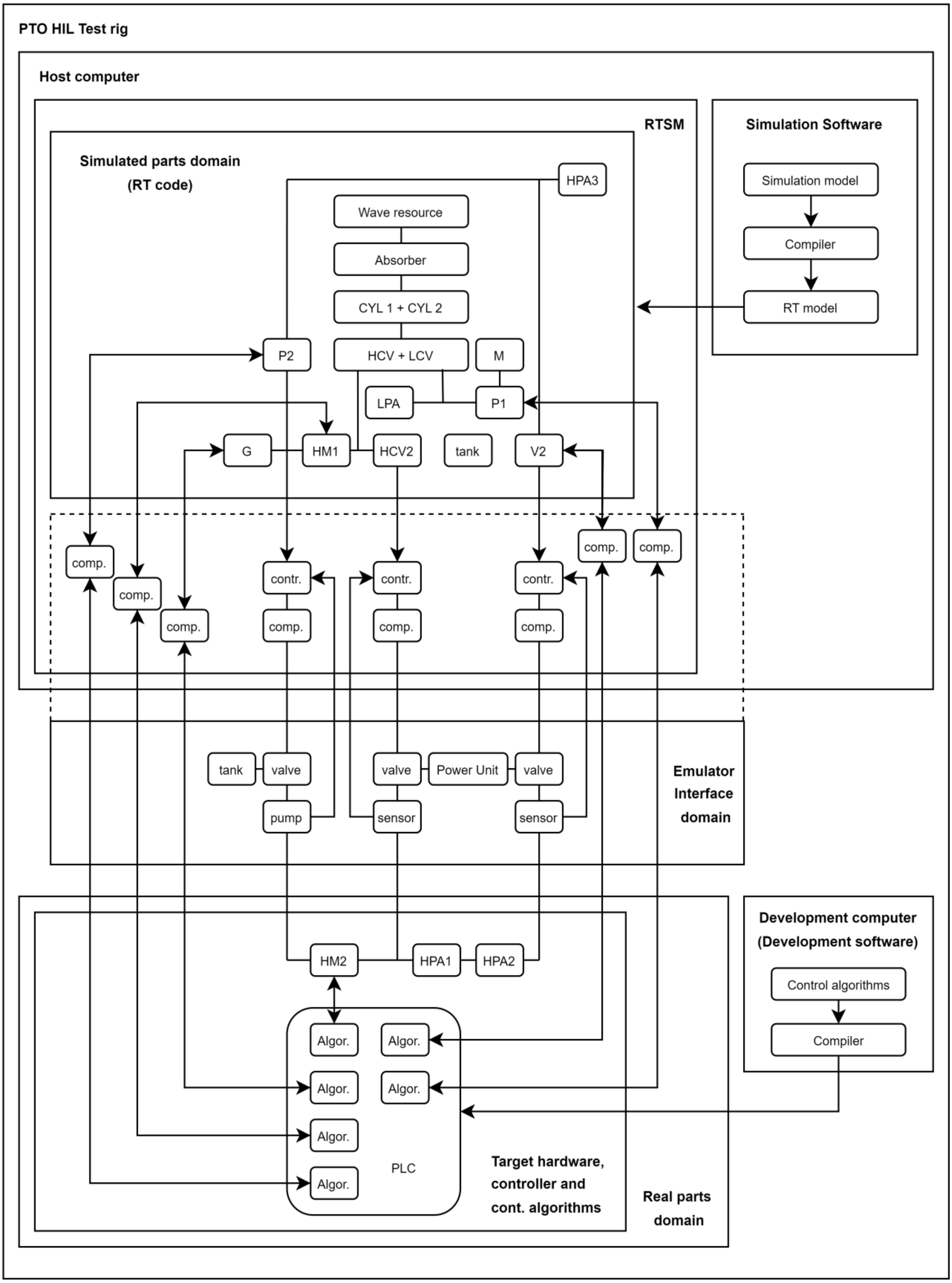

Fig. 12. Representation of the HIL methodology applied to the case study. The terms “contr.”, “comp.” and “Algor.” stand for the controller, interface compensator, and control algorithm, respectively. This framework is present for a target hydraulic motor working as HM2 unit.

The description of the HIL test rig is complemented in the next section with visual representations of the HIL methodology.

IV. PTO HIL SIMULATION FRAMEWORK

The representation of the HIL methodology applied to the case study is presented in Fig. 12. The representation is organized in successive and systematic decompositions that resemble the hierarchical organization of the terms presented in Tables I and II. Accordingly, the PTO HIL test rig is decomposed into the host computer, emulator interface and real parts domain.

The host computer includes software to develop the model of the simulated parts, compile it into an RT model and then load the RT code to the RTSM. The simulated parts domain is shown inside the RTSM with their internal and external functional relations with the emulator interface and target hardware, controller and control algorithms. What is inside the RTSM is only code, however, this representation is intended to give a formal understanding of the HIL methodology, which must be clear to develop actionable representations, such as technical drawings and specifications.

The emulator interface consists of two main parts, control, and actuation. The actuation part implements the physical actions of the simulated parts (HM1, P2, G and V2) on the target hardware (HM2, HPA1, HPA2), target controller (PLC) and target control algorithms and sends feedback signals from the break pump and oil flow sensors to the three emulator controllers. These controllers compare the feedback signals with the ones from the simulated parts and perform corrections on the actuators. Compensators may be included to minimize undesired dynamics added by the emulator system on the HIL testing. The control part is included inside the RTSM. However, it is enclosed inside a dashed line to indicate that belongs to the emulator interface.

Six sets of target controllers and control algorithms are executed inside the PLC, also a target hardware. One set operates directly with the target HM2, whereas all the others with the simulated parts, by the RTSM. Note that the RTSM is not targeting hardware because is not under test. It just executes the RT model and controls the emulator interface, which is not a target hardware as well.

Moreover, additional compensators are provided inside the RTSM to adjust the eventual dynamic effects of the RTSM on HIL testing. Thus, they are also considered as belonging to the emulator interface, since exchange signals with the PLC.

The development computer is inside PLC proprietary development software to develop, compile and load the control algorithms in the PLC controllers.

This HIL representation is expected to evolve as technical problems like communication protocols between devices may lead to adaptations. This is an iterative process, which speeds up as more actionable information is added. However, researchers and developers are expected to keep in mind an overall view of the methodological approach with this HIL formal representation, which is also expected to give them a sense of orientation and purpose, during the implementation process.

V. CONCLUSION

The objective of developing this HIL framework and taxonomy owes to a preliminary search for published work that could help the development of a HIL methodology for the presented case study. It was found, as presented in this paper, that the published work is not clear about the methodology, mostly how is represented and explained, and also to the diversity of the used terminology with similar meanings. This is especially important for researchers interested in applying this technique to their activities, and also, for experienced researchers interested in a more formalized methodology.

The application of the developed methodological framework and taxonomy in the presented case study was easier to apply and the separation between the simulated and real parts, and the interface, is coherent and clear. However, is the first attempt to present a clear and systematic formalization of the HIL methodology in this field of research, as revealed by the literature research. One of the limitations of this study is the reduced number of published case studies from where the framework is developed. However, it is expected that should evolve with further articulations with other case studies in the future.

Research fields always require a research paradigm to advance their activities. It must be based on well-defined and clear methodologies, taxonomy and practices, that may be shared, articulated and developed by the research community. In this sense, this is one of the main objectives of the presented study.

REFERENCES

[1] R. Ahamed, K. McKee, and I. Howard, "Advancements of wave energy converters based on power take-off (PTO) systems: A review," *Ocean Eng.*, vol. 204, p. 107248, May 2020, doi: 10.1016/J.OCEANENG.2020.107248.

[2] J. C. C. Henriques, R. P. F. Gomes, L. M. C. Gato, A. F. O. Falcão, E. Robles, and S. Ceballos, "Testing and control of a power take-off system for an oscillating-water-column wave energy converter," *Renewable Energy*, vol. 85. pp. 714–724, 2016, doi: 10.1016/j.renene.2015.07.015.

[3] C. Liu, Q. Yang, and G. Bao, "Influence of hydraulic power take-off unit parameters on power capture ability of a two-raft-type wave energy converter," *Ocean Eng.*, vol. 150, pp. 69–80, Feb. 2018, doi: 10.1016/J.OCEANENG.2017.12.063.

[4] G. Bacelli, S. J. Spencer, R. G. Coe, A. Mazumdar, D. Patterson, and K. Dullea, "Design and Bench Testing of a Model-Scale WEC for Advanced PTO Control Research" in Proc. of the *12th European Wave and Tidal Energy Conference*, 2017, Cork, Ireland.

[5] N. Delmonte, E. Robles, P. Cova, F. Giuliani, F. Xavier Fäy, J. Lopez, P. Ruol, and L. Martinelli, "An Iterative Refining Approach to Design the Control of Wave Energy Converters with Numerical Modeling and Scaled HIL Testing," *Energies 2020, Vol. 13, Page 2508*, vol. 13, no. 10, p. 2508, May 2020, doi: 10.3390/EN13102508.

[6] H. C. Pedersen, R. H. Hansen, A. H. Hansen, T. O. Andersen, and M. M. Bech, "Design of full-scale wave simulator for testing Power Take off systems for wave energy converters," *Int. J. Mar. Energy*, vol. 13, pp. 130–156, 2016, doi: 10.1016/j.ijome.2016.01.005.

[7] G. Bracco, E. Giorcelli, G. Mattiazzo, M. Raffero, and V. Orlando, "Hardware-In-the-Loop test rig for the ISWEC wave energy system," *Mechatronics*, vol. 25, pp. 11–17, 2015, doi: 10.1016/j.mechatronics.2014.10.007.

[8] T. Aderinto and H. Li, "Ocean Wave Energy Converters: Status and Challenges," *Energies*, vol. 11, no. 5, p. 1250, May 2018, doi: 10.3390/EN11051250.

[9] M. Penalba and J. V. Ringwood, "A review of wave-to-wire models for wave energy converters," *Energies*, vol. 9, no. 7, Jul. 2016, doi: 10.3390/EN9070506.

[10] J. Xie and L. Zuo, "Dynamics and control of ocean wave energy converters," *Int. J. Dyn. Control*, vol. 1, no. 3, pp. 262–276, Sep. 2013, doi: 10.1007/S40435-013-0025-X.

[11] J. F. Gaspar, M. Kamarlouei, R. Pinheiro, M. J. G. C. Mendes, and C. Guedes Soares, "Review on Hardware-In-The-Loop Simulation of Wave Energy Converters," in *Trends in Maritime Technology and Engineering*, 1st ed., C. Guedes Soares and T. A. Santos, Eds. London, UK: CRC Press, 2022, pp. 391–399.

[12] A. D. Shocker and V. Srinivasan, "Multiattribute Approaches for Product Concept Evaluation and Generation: A Critical Review," *J. Mark. Res.*, vol. 16, no. 2, p. 159, 1979, doi: 10.2307/3150681.

[13] E. van Kleef, H. C. M. van Trijp, and P. Luning, "Consumer research in the early stages of new product development: A critical review of methods and techniques," *Food Qual. Prefer.*, vol. 16, no. 3, pp. 181–201, 2005, doi: 10.1016/j.foodqual.2004.05.012.

[14] N. Delmonte, E. Robles, P. Cova, F. Giuliani, F. X. Faÿ J . Lopez, P. Ruol and L. Martinelli "An Iterative Refining Approach to Design the Control of Wave Energy Converters with Numerical Modeling and Scaled HIL Testing," *Energies*, vol. 13, no. 10, p. 2508, May 2020, doi: 10.3390/en13102508.

[15] J. F. Gaspar, M. Kamarlouei, A. Sinha, H. Xu, M. Calvário, F. X. Faÿ E . Robles and C. Guedes Soares, "Speed control of oil-hydraulic power take-off system for oscillating body type wave energy converters," *Renew. Energy*, vol. 97, pp. 769–783, 2016, doi: 10.1016/j.renene.2016.06.015.

[16] G. Moretti, A. Scialò, G. Malara, G. G. Muscolo, F. Arena, R. Vertechy, and M. Fontana, "Hardware-in-the-loop simulation of wave energy converters based on dielectric elastomer generators," *Mecc. 2021 565*, vol. 56, no. 5, pp. 1223–1237, Feb. 2021, doi: 10.1007/S11012-021-01320-8.

[17] A. A. D. Carrelhas, L. M. C. Gato, A. F. O. Falcão, and J. C. C. Henriques, "Control law design for the air-turbine-generator set of a fully submerged 1.5 MW mWave prototype. Part 2: Experimental validation," *Renew. Energy*, vol. 171, pp. 1002–1013, Jun. 2021, doi: 10.1016/J.RENENE.2021.02.128.

[18] A. H. Hansen, M. F. Asmussen, and M. M. Bech, "Hardware-in-the-Loop Validation of Model Predictive Control of a Discrete Fluid Power Power Take-Off System for Wave Energy Converters," *ENERGIES*, vol. 12, no. 19, 2019, doi: 10.3390/en12193668.

[19] T. Hollis, H. B. Karayaka, Y. H. Yu, and Y. Yan, "Hardware-in-the-Loop Simulation for the Proposed Slider-Crank Wave Energy Conversion Device," *Ocean. 2018 MTS/IEEE Charleston, Ocean 2018*, pp. 1–7, 2019, doi: 10.1109/OCEANS.2018.8604770.

[20] M. Neshati, G. Curioni, H. R. Karimi, and J. Wenske, "H∞ drive train control for hardware-in-the-loop simulation with a scaled dynamometer test bench," *vol. 2017-Janua. Institute of Electrical and Electronics Engineers Inc., 2017*, pp. 8578–8583.

[21] U. Sancar, A. O. Onol, A. Onat, and S. Yesilyurt, "Hardware-in-the-loop simulations and control design for a small vertical axis wind turbine," in *2015 XXV International Conference on Information, Communication and Automation Technologies, (ICAT)*, 2015, pp. 1–7, doi: 10.1109/ICAT.2015.7340497.

[22] L. Huijgens, A. Vrijdag, and H. Hopman, "Hardware in the loop experiments with ship propulsion systems in the towing tank: Scale effects, corrections and demonstration," *Ocean Eng.*, vol. 226, p. 108789, Apr. 2021, doi: 10.1016/j.oceaneng.2021.108789.

[23] R. O. Berriel, M. Shadman, Z. Wu, R. F. S. Dias, R. M. Stephan, and S. F. Estefen, "Hardware-in-the-loop development of a heaving point absorber wave energy converter using inertia emulation," *Electr. Eng. 2021*, pp. 1–10, Mar. 2021, doi: 10.1007/S00202-021-01244-2.

[24] T. Puleva, G. Rouzhekov, T. Slavov, and B. Rakov, "Hardware in the loop (HIL) simulation of wind turbine power control," in *Mediterranean Conference on Power Generation, Transmission, Distribution and Energy Conversion (MedPower 2016)*, 2016, pp. 1–8, doi: 10.1049/cp.2016.1053.

[25] H. B. Karayaka, Y.-H. Yu, and E. Muljadi, "Investigations into Balancing Peak-to-Average Power Ratio and Mean Power Extraction for a Two-Body Point-Absorber Wave Energy Converter," *Energies 2021, Vol. 14, Page 3489*, vol. 14, no. 12, p. 3489, Jun. 2021, doi: 10.3390/EN14123489.

[26] Castellini, L., Gallorini, F., Alessandri, G., Alves, E.F., Montoya, D., Mudigonda, B. and Tedeschi, E., "Comparison of Offline, Real-Time Models and Hardware-in-the-Loop Test Results of a Power Take-Off for Wave Energy Applications". *Journal of Marine Science and Engineering*, Vol 10, No. 11, p.1744, 2022.

[27] C. Signorelli, C. Villegas, and J. Ringwood,."Hardware-in-the-loop simulation of a heaving wave energy converter", In *Proceedings of the 9th European Wave and Tidal Energy Conference (EWTEC)*. 2011.

[28] A. Haas, B. Schrage, G. Menze, P. M. Sieberg, and D.

Schramm, "Improvements on the Dynamical Behavior of a HiL-Steering System Test Bench," Actuators, Vol. 12, No. 5, p. 186, 2023, doi: 10.3390/act12050186.

[29] "dSPACE 1104 Controller Board", https://www.dspace.com/en/inc/home/products/hw/singbord/ds1104.cfm, (accessed Jun. 28, 2023).

[30] N. Altin, and I. Sefa, “dSPACE based adaptive neuro-fuzzy controller of grid interactive inverter,” *Energy Conversion and Management*, Vol. 56, pp. 130–139, 2012.

[31] "What is CompactRIO?", https://www.ni.com/pt-pt/shop/compactrio.html, (accessed Jun. 28, 2023).

[32] "Speedgoat Real-Time Target Machine", https://www.speedgoat.com/products-services/real-time-target-machines, (accessed Jun. 28, 2023).

[33] “Raspberry Pi”, https://www.raspberrypi.com, (accessed Jun. 28, 2023).

[34] “FPGA Fundamentals: Basics of Field-Programmable Gate Arrays”, https://www.ni.com/pt-pt/shop/electronic-test-instrumentation/add-ons-for-electronic-test-and-instrumentation/what-is-labview-fpga-module/fpga-fundamentals.html; (accessed Jun. 30, 2023)

[35] “AMD XILINX”, https://www.xilinx.com/products/silicon-devices/fpga/what-is-an-fpga.html, (accessed Jun. 30, 2023)

[36] M. Calvario, J. F. Gaspar, M. Kamarlouei, T. S. Hallak, and C. Guedes Soares, “Oil-hydraulic power take-off concept for an oscillating wave surge converter”. *Renewable Energy. 2020*, 159:1297-1309.